Synthesis and characterization of thermally evaporated $(Bi,Sb)_2S_3$ thin films

K. KANDASWAMY[a], P. CHRISTOPHER SELVIN[a*], B. NALINI[b], I. MOHAMED ABDULLA[a], K. P. ABHILASH[a]
[a]*Department of Physics, NGM College, Pollachi-642001, Tamil Nadu, India*
[b]*Department of Physics, Avinashilingam University, Coimbatore -641043, India*

Thin films of$(Bi,Sb)_2S_3$ were deposited on a glass substrate by vacuum thermal evaporation method and annealed at different temperatures. The elemental compositions of the as-deposited and annealed films were confirmed by energy dispersive X-ray analysis (EDAX). The prepared films were structurally and morphologically characterized by X-ray diffraction (XRD) and microscopic (SEM & AFM) techniques respectively. It has been confirmed that the films posses polycrystalline structure with orthorhombic phase and the crystallite size of the films vary from 28 to 63 nm. The observed band-gap energies of the films varying from 2.05 eV to 2.11 eV and its temperature dependence were estimated from optical absorption measurements. Dielectric study shows a decrease in dielectric loss with increase in temperature. The dielectric properties of the films were studied using two probe techniques. The electrical resistivity reveals the semiconducting nature of the film.

(Received July 28, 2014; accepted January 21, 2015)

Keyword: Bismuth antimony trisulfide nano films, EDAX, XRD, Optical absorption, Bandgap, Semiconductor

1. Introduction

The chalcogenide thin films have received considerable attention in recent years because of their world wide applications in various fields of science and technology [1,2]. Especially Group V-VI compound thin films have potential applications in optoelectronic devices, photo electrochemical devices, thermoelectric coolers [3], solar selective materials, decorative coatings, etc[4]. Generally the binary alloys such as Sb_2S_3 are covalent in nature and the addition of the third element Bi creates iono-covalent bonds and as a result the conduction increases [5]. This makes Bi an important candidate to improve the electrical and optical properties of $(Bi,Sb)_2S_3$ thin films. At present particularly $(Bi,Sb)_2S_3$ alloy is found to be the best material for thermoelectric cooling. Since Nayak et al had reported the preparation and characterization of $Bi_{2-x}Sb_xS_3$ thin films coated by dip-dry process [6], many similar reports on this material started appearing with different compositions and deposition techniques [7-11].

Vacuum thermal evaporation of preparing thin films is an important and versatile technique for functional coatings with the advantages such as low contamination (high chemical purity), high film deposition rate, improved control of deposition, ultra- thin layer formation etc. There is not much work done on the vacuum thermal evaporation of $(Bi,Sb)_2S_3$ thin films. Hence, an attempt has been made to prepare thin films of $(Bi,Sb)_2S_3$ by vacuum thermal evaporation method. The present study reports the structural, optical and electrical characterization of thermally evaporated $(Bi,Sb)_2S_3$ thin films. It has been reported that annealing is necessary to remove the defects for such thermoelectric thin films to improve their properties [12]. Annealing effects on the structural, optical, electrical properties of $(Bi,Sb)_2S_3$ are also analyzed and reported here.

2. Experimental

Bulk alloy of $(Bi,Sb)_2S_3$ was prepared by melting the high purity elements taken in the stoichiometric ratio in a vacuum sealed ($1x10^{-3}$ Torr) quartz ampule by heating in a rotating furnace at 1098K for 24 hours. The crystallization temperature (T_c) of the alloy was carried out using differential scanning calorimeter (NETZSCH DSC 204 F1) at a heating rate of 35/20.0(K/min) with a precision of ±1 K [11]. To prepare thin films, the alloy of $(Bi,Sb)_2S_3$ was deposited on well cleaned glass substrates held at room temperature (300K) with thickness 188nm by vacuum thermal evaporation method (using *HIND HIVAC 12AD4M*) at a pressure of about 2 $x10^{-5}$ Torr. The thickness and rate of deposition (2 to 3 Å/sec) of the films were determined by using a quartz crystal monitor. The films were annealed in an open atmosphere for one hour at two different temperatures (533K and 553K).

Energy dispersive X-ray analysis (EDAX) studies reveal the elemental composition of the as deposited and annealed films. The structural studies were analyzed by X-ray diffractometer (RIGAKU) using CuKα (λ=1.5418A^0) radiation, the particle size was confirmed using SEM (JEOL MODEL 6300(LA)). The AFM nanoscope (Model-NSE, Serial no-245) was used to probe different portion of the surface in-contact. The optical absorption studies and dielectric property of the films were carried out using UV-Vis-NIR Spectrophotometer (CARY5E) and LCR Meter (HIOKI 3532-50) respectively.

3. Results and Discussion

3.1 DSC Analysis

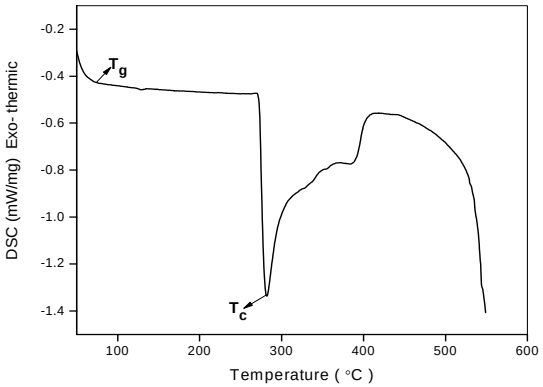

Fig. 3.1. DSC curve for $(Bi,Sb)_2S_3$ alloy

Fig. 3.1 shows the characteristic DSC curve of the $(Bi,Sb)_2S_3$ alloy. The glass transition temperature, Tg, is defined as the temperature that shows an endothermic step in the DSC curve. The crystallization temperature Tc, refers to the onset temperature of crystallization of the considered glass. From fig.3.1 it can be seen that the characteristic glass transition temperature (*T*g) and the crystallization temperature (Tc) of the $(Bi,Sb)_2S_3$ alloy is 353K and 553K respectively and the stability factor **S** (*T*c –*T*g) is 200K [13].

3.2 XRD analysis

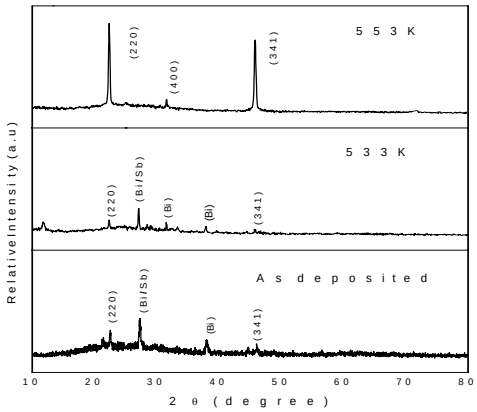

Fig. 3.2. XRD patterns of $(Bi,Sb)_2S_3$ thin films with a thickness of 188 nm

Fig. 3.2 shows the XRD patterns of $(Bi,Sb)_2S_3$ thin films of thickness 188nm. The observed peaks 2θ = 22.38°, 33.10°, and 46.60° were matched with the standard JCPDS data (File. No. 37-0917) which corresponds to the planes (2 2 0), (4 0 0) and (3 4 1) respectively. The XRD pattern of $(Bi,Sb)_2S_3$ at room temperature and annealed at 533K, shows some of the peaks due to Bi/Sb which prevails from the parent compound shows an incomplete formation of $(Bi,Sb)_2S_3$ phase. But the film annealed at 553K showed the complete formation of $(Bi,Sb)_2S_3$ orthorhombic polycrystalline structure which could be substantiated by the DSC results which showed the crystallization temperature of $(Bi,Sb)_2S_3$ alloy material 553K. The crystallite size (D) was calculated using Debye-Scherrer's formula

$$D = \frac{k\lambda_x}{\beta \cos\theta} \quad (1)$$

where 'k' is the Scherrer's constant, λ_x is the wavelength of the X-ray used, 'β' is the full width half maximum (FWHM) and θ is the Bragg's angle. The calculated crystallite size of the $(Bi,Sb)_2S_3$ films are 27.92nm, 36.92nm and 49.62nm for the as deposited, annealed at 533K and 553K respectively.

The dislocation density (δ) of the polycrystalline thin films has been evaluated [14] from the formula,

$$\delta = \frac{1}{D^2} \quad (2)$$

and found to vary between 0.25 x 10^{15} and 1.28 x 10^{15} lines/m^2.

3.3 Morphological analysis

Fig. 3.3 shows the elemental composition of the as deposited and annealed $(Bi,Sb)_2S_3$ films [15]. The presence of Bi, Sb and S were confirmed by EDAX analysis and their atomic weight percentages were tabulated. The stochiometry of the film is more or less maintained in the prepared samples. The elemental composition of the sample shows some variation from the stochiometry.

Table 1 Elemental composition of $(Bi,Sb)_2S_3$ films

Element	Atom %		
	As deposited	533K	553K
S	39.29	38.47	36.04
Sb	25.09	25.07	23.44
Bi	35.62	36.46	40.52
Total	100.00	100.00	100.00

As evidenced from the EDX analysis, as deposited sample shows the elemental composition of $Bi_{0.78}$ $Sb_{0.95}S_{4.1}$ which changes to the compositions $Bi_{0.8}$ $Sb_{0.95}S_{4.08}$ and $Bi_{0.89}$ $Sb_{0.88}S_{3.83}$ when annealing to the temperatures 533K and 553 K respectively.

The microstructure and morphology of the as deposited and annealed $(Bi,Sb)_2S_3$ films of thickness 188nm were carried out using scanning electron microscopy (SEM) and atomic force microscopic (AFM) studies [16,17]. The SEM images (Fig.3.4) show that the

films are almost homogeneous in nature without any pinholes or cracks and covers the substrate well. But with increase in the annealing temperature the inhomogeneity also appears to increase. The AFM images (Fig.3.5) also support the result. The particle size calculated from the SEM images are in the order of 60, 70 and 80 nm for the as deposited, annealed at 533K and 553K respectively. This clearly shows that the particle size increases with the increase in annealing temperature. The particle size is slightly larger than the size estimated by the Scherrer's formula calculations based on XRD pattern. The discrepancy between SEM and XRD results divulge that the prepared samples are polycrystalline in nature [18].

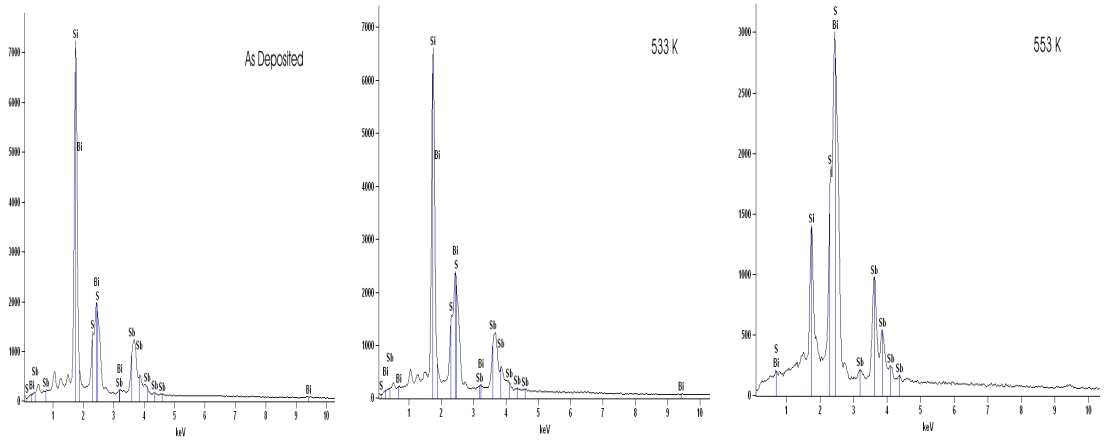

Fig. 3.3. Chemical composition of $(Bi,Sb)_2S_3$ thin films with thickness 188nm (a) As deposited (b) 533K (c) 553K

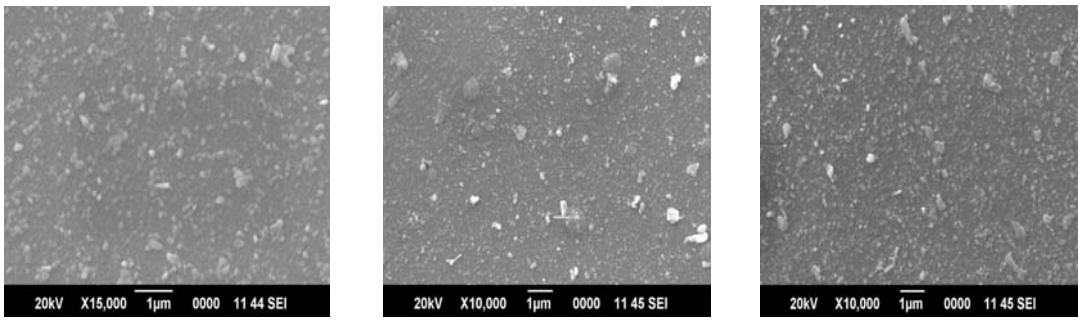

Fig. 3.4. SEM images for $(Bi,Sb)_2S_3$ thin films thickness 188nm (a) as deposited (b) annealed at 533K (c) annealed at 553K

3.4 AFM analysis

Atomic force microscopy (AFM) was used to examine the surface morphology of $Bi(Sb_2S_3)$ thin films. Fig.3.5 (a,b,c) shows the AFM micrographs of the films of as deposited, annealed (at 533K and 553K) thin films. According to the definition, the root mean square value of roughness [8] is given by the equation,

$$RMS = \frac{1}{\sqrt{n}} \sqrt{\sum_{I=1}^{n} (x_0 - x_i)^2} \qquad (3)$$

where x_i is the individual AFM data point, n is the number of data points and x_0 is their mean value given by

$$x_0 = \frac{\sum_{i=1}^{n} x_i}{n} \qquad (4)$$

Automatically calculated root mean square value of roughness was found to be 18.2, 21.4 and 54.1 nm for the films of as deposited, annealed at 533K and 553K respectively [5].

The as deposited and annealed films resulted in blunt ended rough surface with average protrusions of ~100nm above the RMS value of roughness for the scanned surface. The film annealed at 533K found to possess better morphology as revealed by AFM images with ~100nm protrusions above the RMS value of the resulted surface indicating that the former one was under developed by morphology. Further increment in annealing temperature

(553K) resulted in inhomogeneous roughness at specific locations with a protrusion of ~300nm about the RMS value of the scanned surface which is the most probable and reported in microstructures.

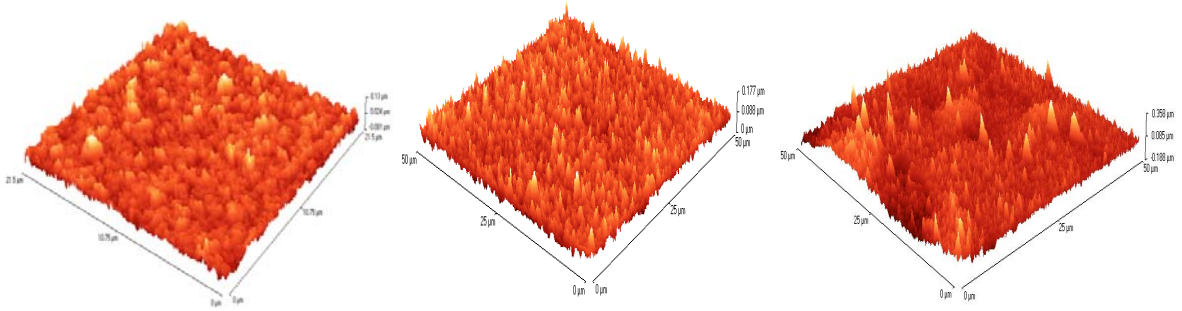

Fig. 3.5. AFM images for (Bi, Sb)$_2$S$_3$ thin films 188nm
(a) as deposited (b) annealed at 533K (c) annealed at 553K

3.5 Optical studies

Fig. 3.6 shows the reflectance spectra of the as deposited and annealed $(Bi,Sb)_2S_3$ films in the wavelength range 350 – 790nm. Reflectance of the incident light is increased for samples annealed at higher temperatures. The absorption coefficient α is calculated from the reflectance spectra of $Bi(Sb_2S_3)$ films. The nature of the transition (direct or indirect) was determined by using the relation

$$\alpha = \frac{A(h\nu - E_g)^{\rho}}{h\nu} \qquad (5)$$

where, A is a constant and ρ assumes values of $^1/_2$, 2, $^3/_2$ and 3 for allowed direct, allowed indirect, forbidden direct and forbidden indirect transitions, respectively. The $(Bi,Sb)_2S_3$ thin film exhibits the behavior of allowed direct transition. The plots of $\alpha h\nu^2$ Vs hν is a straight line whose intercept on energy axis gives the band gap energy E_g as shown in figure 3.7.

The bandgap energy of the $(Bi,Sb)_2S_3$ thin film is found to be 2.11eV, 2.09 eV and 2.05 eV for the films of as deposited, annealed at 533K and 553K respectively.

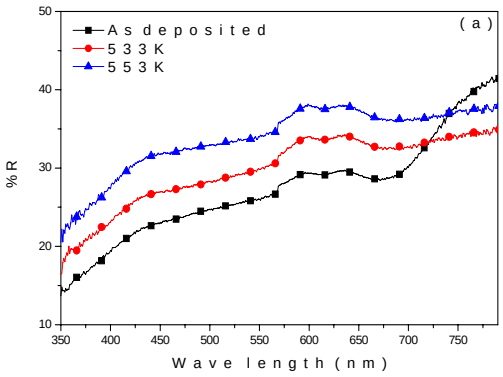

Fig. 3.6. Reflectance Spectra of (Bi,Sb)$_2$S$_3$ films

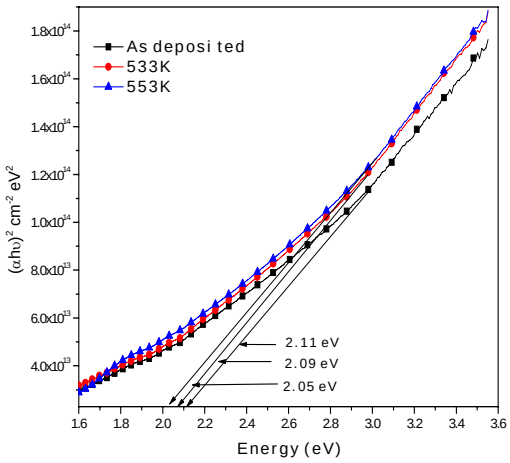

Fig. 3.7. The plots for $\alpha h\nu^2$ vs hν for the thickness 188nm

3.6 Dielectric studies

In the present investigation dielectric constant of $(Bi,Sb)_2S_3$ thin film capacitors prepared by vacuum evaporation technique have been calculated at different temperature over a frequency range of 800 Hz to 200 KHz.

The variation of capacitance with frequency at different temperatures for $(Bi,Sb)_2S_3$ films with thickness 188nm is shown in fig. 3.8. Initially the capacitance shows a slight increase as frequency increases. Further increase in frequency shows no change in the capacitance. The dielectric properties of $(Bi,Sb)_2S_3$ thin films shows an increase in capacitance with increase in annealing temperatures. [14,17,19,20].

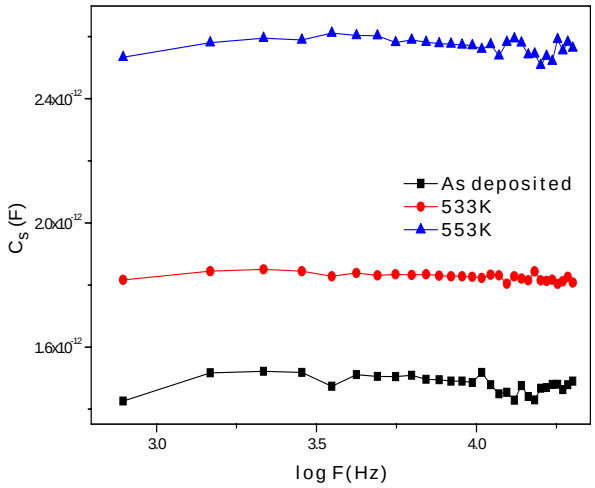

Fig. 3.8. Variation of capacitance with frequency for $(Bi,Sb)_2S_3$ thin films

The sample annealed at 553K shows higher capacitance. From the XRD result, it is evident that The sample annealed at 553K which shows better crystallinity from the XRD data shows higher capacitance.

The variation of dielectric loss factor **(tan δ)** with frequency at different temperature for vacuum annealed $(Bi,Sb)_2S_3$ films are shown in Fig 3.9. Up to the log frequency 3.6, the tanδ curve shows regular behavior after which it shows an irregular behavior in dielectric loss. The higher temperature annealing decreases the dielectric loss [14].

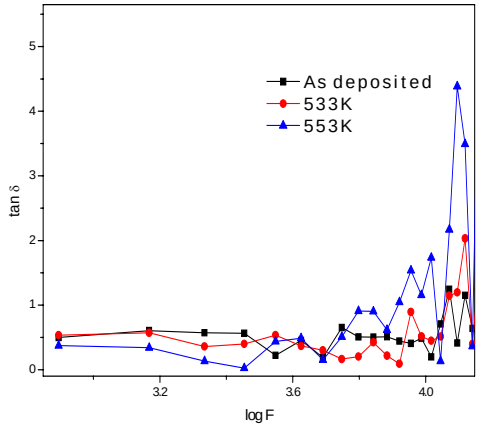

Fig. 3.9. Variation of tan δ with frequency of $(Bi,Sb)_2S_3$ thin films

The dielectric constant (ε') was evaluated from the knowledge of capacitance (C), film thickness (d), free space permittivity (ε_0) and area of the capacitor (A), using the relation

$$Cd = \varepsilon' \varepsilon_o A \qquad (6)$$

Fig. 3.10 shows the variation of dielectric constant with frequency at various temperatures. Temperature does not affect the process of electric polarization in non-polar dielectrics. The nature of dependence of permittivity on temperature in solid ionic dielectric may be different and in most cases the ionic mechanism of polarization will be observed and dielectric constant(ε') would increases with the increase in temperature which may be due to increase in crystallite size of the films [14].

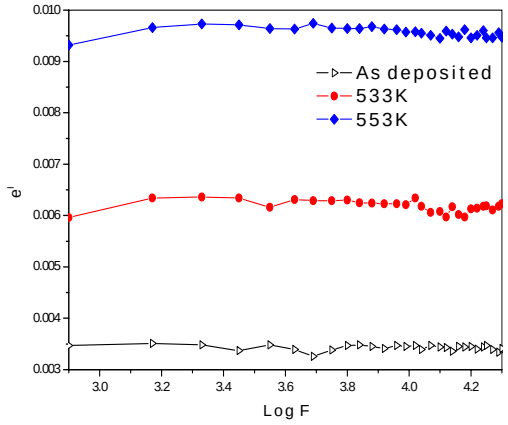

Fig.3.10. Variation of dielectric constant with frequency (a) As deposited (b) annealed at 533K (c) annealed at 553K

3.7 Electrical Resistivity

Fig 3.11 shows the Arrhenius plot of $(Bi,Sb)_2S_3$ thin films with thickness 188nm. The electrical resistivity measurement of $(Bi,Sb)_2S_3$ thin film reveals semiconducting behavior, as resistivity decreases almost exponentially with increase in temperature following the Arrhenius behavior. [13,21,22].

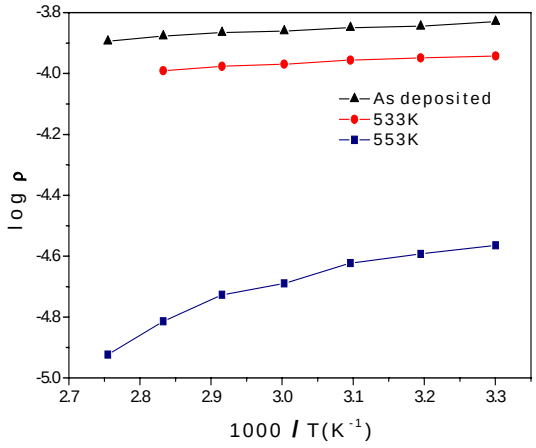

Fig. 3.11 Variation of log ρ vs. temperature of $(Bi,Sb)_2S_3$ thin films

4. Conclusion

The $(Bi,Sb)_2S_3$ thin films were prepared by vacuum thermal evaporation method which was polycrystalline with orthorhombic phase. The crystallite size of the films was found to increase with increasing annealing temperature. Annealing effect of the films at higher temperature resulted in better crystallinity which was confirmed by XRD analysis. The film annealed at 553 K showed the complete formation of $(Bi,Sb)_2S_3$ orthorhombic polycrystalline structure which could be substantiated by the DSC results which showed the crystallization temperature of $(Bi,Sb)_2S_3$ alloy material 553 K. The SEM images showed that the films are almost homogeneous in nature without any pinholes or cracks and cover the substrate well. But with increase in the annealing temperature the inhomogeneity was generated. The presence of Bi, Sb and S were confirmed by EDAX analysis.

The AFM results showed that the as deposited and annealed films resulted in blunt ended rough surface with average protrusions of ~100nm above the RMS value of roughness for the scanned surface. Among the films studied with various temperatures, the film annealed at 533K found to possess better morphology as revealed by AFM images.

From the optical analysis, it has been ascertained that the optical transitions are direct and allowed type. It has been confirmed that the bandgap energy decreases with increase in annealing temperature due to the expansion occurred in the crystallite size.

The dielectric properties of $(Bi,Sb)_2S_3$ thin films shows an increase in capacitance with increase in annealing temperatures. The sample annealed at 553 K which shows better crystallinity from the XRD data shows higher capacitance.

The electrical resistivity measurement of $(Bi,Sb)_2S_3$ thin film reveals semiconducting behavior, as resistivity decreases almost exponentially with increase in temperature following the Arrhenius behavior.

References

[1] K. Rajasekar, A. Subbarayan, R. Sathyamoorthy, Sol Energ Mat Sol C, **90,** 2515 (2006)
[2] N.S. Yesugade, C.D. Lokhande, C.H. Bhosale, Thin Solid Films, **263,** 145 (1995)
[3] Zishan H. Khan, M. Zulfequar, M. Ilyas, M. Husain, Kh. Selima Begam, Curr Appl Phys, **2,** 167 (2002)
[4] B.B. Nayak, H.N. Acharya, G.B. Mitra, B.K. Mathur, Thin Solid Films, **105,** 17 (1983)
[5] R.H. Bari, L.A. Patil, Indian J Pure Ap Phy, **48** 127 (2010).
[6] V.A. Patil, A.R. Patil, J.W. Choi, D.S. Paik S.J. Yoon, Surf Eng., **23** 28 (2007)
[7] Padiyan. D, S. Subramanian, P. Chithralekh. J Pathinettam Non-Cryst Solids. **356,** 1173 (2010)
[8] J. Deepa, R. Sathyamoorthy, A. Subburayan, S.Velumani, P.J. Sebastian, R. Perez, Sol Energ Mat Sol C, **88,** 187 (2005)
[9] P.G. Ganesan, V. Damodara Das, Mater Lett **60,** 2059 (2006)
[10] N. Tigau, V. Ciupina, G .Prodan, G.I. Rusu, C. Gheorghies, E. Vasile, J. Optoelectron Adv. Mater **5,** 907 (2003)
[11] V.A. Patil, A.R. Patil, J.W. Choi, D.S. Palk, S.J. Yoon,Surf Eng. **23,** 28 (2007)
[12] J.D. Musgraves, N. Carlie, J. Hu, L. Petit, A. Agarwal, Acta Mater, Volume **59** 5032 (2011).
[13] Rachid Makhloufi, Ahmed Boutarfaia, Marcel Poulain, J Alloy Compd **398,** 249 (2005) .
[14] Haitao Guo, Haizheng Tao, Yueqiu Gong, Xiujian Zhao, J Non-Cryst Solids **354**, 1159 (2008).
[15] Xuebo Cao, Li Gu, Wancheng Wang, Weijian Gao,Lanjian Zhuge, Yahong Li, J cryst growth **286,** 96 (2006).
[16] Kamal R. Chowdhari, Amay, P. Wadawale, Shamile, Ghoshal, Suresh, M. Chopade,V.S Sagoria, Vimal K, Inorg Chem acta. **363** 375 (2010)
[17] V Narayanan, Sawant, Jasmine B, Biswal, Shivram S, J Coord Chem Acta.Volume **64,** 1758 (2011)
[18] Emerson R. Camargo, Cristiano M. Barrado, Caue Ribeiro, Elson Longo R. Lcite, J Alloy and Compd**. 475** 817 (2009)
[19] B.Li,L.Wang,B.Kang,P.Wang,Y.Qiu, Sol Energ Mat Sol C **90** 2515 (2006)
[20] I. K.El Zawawi, A. Abel-Moez, F.S. Terra, M. M. Mounir, Thin Solid Film **324** 300 (1998)
[21] N. Jessy Mathew, Rachel Oommen, Usha Rajalakhsmi, Chalcogenide letters, **8,** 701(2011).
[22] P.G.Ganesan, P. Damodara das,Mater Lett **60,** 2059 (2006)
[23] V. Damodara das, S. Selvaraj, Mater Chem Phys **62,** 68 (2000)

*Corresponding author: pcsphyngmc@rediffmail.com